



# Directing stem cell fate on hydrogel substrates by controlling cell geometry, matrix mechanics and adhesion ligand composition



Junmin Lee, Amr A. Abdeen, Douglas Zhang, Kristopher A. Kilian\*

Department of Materials Science and Engineering, University of Illinois at Urbana-Champaign, IL 61801, USA

## ARTICLE INFO

### Article history:

Received 28 June 2013

Accepted 21 July 2013

Available online 7 August 2013

### Keywords:

Mesenchymal stem cells  
Microcontact printing  
Microenvironment  
Differentiation  
Polyacrylamide hydrogels

## ABSTRACT

There is a dynamic relationship between physical and biochemical signals presented in the stem cell microenvironment to guide cell fate determination. Model systems that modulate cell geometry, substrate stiffness or matrix composition have proved useful in exploring how these signals influence stem cell fate. However, the interplay between these physical and biochemical cues during differentiation remains unclear. Here, we demonstrate a microengineering strategy to vary single cell geometry and the composition of adhesion ligands — on substrates that approximate the mechanical properties of soft tissues — to study adipogenesis and neurogenesis in adherent mesenchymal stem cells. Cells cultured in small circular islands show elevated expression of adipogenesis markers while cells that spread in anisotropic geometries tend to express elevated neurogenic markers. Arraying different combinations of matrix protein in a myriad of 2D and pseudo-3D geometries reveals optimal microenvironments for controlling the differentiation of stem cells to these “soft” lineages without the use of media supplements.

© 2013 Elsevier Ltd. All rights reserved.

## 1. Introduction

Cells adhering to the extracellular matrix (ECM) can sense the mechanical properties through specific interactions of cell surface integrins with adhesion ligands [1–5]. Traction forces exerted by the cell through these interactions influence cytoskeletal tension and lead to changes in cell shape and associated signaling cascades that ultimately regulate gene expression [6–10]. This process of mechanotransduction has emerged as an important aspect of stem cell differentiation and is dependent on both the mechanics and the composition of the microenvironment. For example, Datta et al. revealed the importance of the mechanical and biochemical microenvironment by culturing osteoprogenitor cells on a decellularized osteoblast matrix leading to increased expression of osteogenic markers [11]. Work in the Schaffer and Healey groups has demonstrated that mechanical properties can guide neurogenesis in neural stem cells where softer matrices promote dendritic process extension [12]. A study by Engler, Discher and colleagues demonstrated the importance of matrix mechanics in guiding MSC fate by studying cells adherent to collagen-coated polyacrylamide hydrogels of variable stiffness [8]. MSCs were found to commit to lineages based on the similarity to the committed

cells' native matrix; soft polyacrylamide gels (<1 kPa) promote neurogenesis, intermediate stiffness gels (~10 kPa) promote myogenesis and stiff gels (>30 kPa) promote osteogenesis.

In addition to stiffness, the composition and presentation of adhesion ligands on a substrate have been shown to influence MSC differentiation [1–3,13–15]. Cooper-White and co-workers demonstrated that different matrix proteins — collagen, fibronectin and laminin — grafted to hydrogel substrates of different stiffness will significantly influence the expression of myogenic and osteogenic markers. This work suggests that the identity of adhesion ligand and its presentation to the cell can play an important role in promoting competing differentiation outcomes. Kilian and Mrksich recently showed how the density and affinity of surface bound adhesion peptides could modulate the expression of markers associated with neurogenesis, myogenesis and osteogenesis, further confirming the importance of the type and presentation of ligand in guiding stem cell differentiation [3].

Another important physical parameter that has emerged as an important cue in guiding the differentiation of stem cells, and is influenced by stiffness and the presentation of adhesion ligands, is cell shape [4,16–19]. For instance, Chen and colleagues demonstrated that MSCs captured on small islands tended to prefer adipocyte differentiation when exposed to a mixture of osteogenic and adipogenic soluble cues while cells captured on large islands developed a higher degree of cytoskeletal tension and preferred to

\* Corresponding author.

E-mail address: [kakilian@illinois.edu](mailto:kakilian@illinois.edu) (K.A. Kilian).

adopt an osteoblast outcome [16]. In a related study, Kilian et al. demonstrated that MSCs patterned in geometries with subcellular concave regions and moderate aspect ratios increase the actomyosin contractility of the cell and promote osteogenesis [17]. In both of these studies, keeping cell shape the same across a population of MSCs was shown to normalize the differentiation outcome when compared to unpatterned cells that take on a host of different geometries.

An important lesson that has emerged from these studies is that there is clearly interplay between matrix mechanics, adhesion ligand presentation and cell geometry during differentiation [4,5,20]. The majority of research efforts have focused on varying one physical cue while exploring the influence on biological activity. However, *in vivo* cell fate is likely influenced by a combination of geometry, mechanics and ECM composition [21,22]. Thus we reasoned that combining these cues would prove useful in designing materials that more closely emulate the *in vivo* microenvironment and “fine-tune” a desired differentiation outcome.

In this paper, we use soft lithography to micropattern multiple matrix proteins — alone and in combinations — on hydrogel substrates with the mechanical properties of soft tissue to explore the physical and biochemical cues that guide MSCs towards adipogenesis and neurogenesis outcomes. Immunofluorescence staining and real-time PCR are employed to assess the expression of key markers during differentiation. We explore the translation of our findings to a pseudo-3D hydrogel format that more closely represents the *in vivo* environment.

## 2. Materials and methods

### 2.1. Materials

Laboratory chemicals and reagents were purchased from Sigma Aldrich unless otherwise noted. Tissue culture plastic ware was purchased from Fisher Scientific. Cell culture media and reagents were purchased from Gibco. Human MSCs and differentiation media were purchased from Lonza and produced by Osiris Therapeutics. Mouse anti- $\beta$ 3 tubulin was purchased from Sigma (T8660), rabbit anti-PPAR $\gamma$  was purchased from Cell Signaling (C26H12), and chicken anti-MAP2 was purchased from abcam (ab5392) Technologies. Tetramethylrhodamine-conjugated anti-rabbit IgG antibody, Alexa Fluor 647-conjugated anti-mouse IgG antibody, Alexa488-phalloidin and 4',6-diamidino-2-phenylindole (DAPI) were purchased from Invitrogen. Glass coverslips (18-mm circular) for surface preparation were purchased from Fisher Scientific. These cells were derived from bone marrow isolated from the iliac crest of human volunteers. MSCs were tested for purity by Lonza, and were positive for CD105, CD166, CD29, and CD44, negative for CD14, CD34, and CD45 by flow cytometry, and had ability to differentiate into osteogenic, chondrogenic, adipogenic lineages (<http://www.lonza.com>). The use of human MSCs in this work was reviewed and approved by the University of Illinois at Urbana-Champaign Biological Safety Institutional Review Board.

### 2.2. Polyacrylamide gel fabrication and protein immobilization

We used the protocol of making  $0.48 \pm 0.16$  kPa gels by using the mixture of 3% of Acrylamide and 0.06% of Bis-acrylamide, and for the polymerization, 0.1% of Ammonium Persulfate (APS) and Tetramethylethylenediamine (TEMED). Hydrazine hydrate 55% (Fisher Scientific) was utilized for 1 h to convert amide groups in polyacrylamide to reactive hydrazide groups. Sodium periodate (Sigma-Aldrich) was incubated with the glycoproteins to yield free aldehydes. The gels were washed for 1 h in 5% glacial acetic acid (Fluka/Sigma) and for 1 h in distilled water. To create patterned surfaces, polydimethylsiloxane (PDMS, Polysciences, Inc.) stamps were fabricated by polymerization upon a patterned master of photoresist (SU-8, MicroChem) created using UV photolithography through a laser printed mask. 25  $\mu$ g/mL of fibronectin, laminin, or type 1 collagen (for combinations of ligands, the final concentration was normalized to 25  $\mu$ g/mL) in PBS was applied for 30 min to the top of patterned or unpatterned PDMS, and then dried under air, and applied to the surface. Pseudo-3D microwells were fabricated by templating the polyacrylamide gels on an SU-8 photolithography master displaying the inverse features used in fabricating the PDMS stamps. After subjecting the microwells to hydrazine treatment and oxidized protein, adhesive tape was applied to the gel and removed quickly to shear off the top layer of protein-conjugated gel.

### 2.3. Cell culture

Human mesenchymal stem cells (MSCs) were thawed from cryopreservation (10% DMSO) and cultured in Dulbecco's Modified Eagle's Medium (DMEM) low glucose (1 g/mL) media supplemented with 10% fetal bovine serum (MSC approved FBS; Invitrogen), and 1% penicillin/streptomycin (p/s). Media was changed every 4 days and cells were passaged at nearly 80% confluency using 0.25% Trypsin:EDTA (Gibco). Passage 4–7 MSCs were seeded on patterned and non-patterned surfaces at a cell density of  $\sim 5000$  cells/cm<sup>2</sup>.

### 2.4. Immunofluorescence and histology

After incubation for 10 days, surfaces were fixed with 4% formaldehyde (Ted Pella, Inc.) for 20 min, and cells were permeabilized in 0.1% Triton X-100 in PBS for 30 min and blocked with 1% bovine serum albumin (BSA) for 15 min. Primary antibody labeling was performed in 1% BSA in PBS for 1 h at room temperature (20 °C) with rabbit anti-PPAR $\gamma$  (Cell Signaling Tech., 1:200 dilution) or MAP2 (Santa Cruz, 1:200 dilution) and mouse anti- $\beta$ 3 Tubulin (abcam, 1:200 dilution). Secondary antibody labeling was performed using the same procedure with tetramethylrhodamine-conjugated anti-rabbit IgG antibody and Alexa Fluor 647-conjugated anti-mouse IgG antibody (1:200 dilution) along with Alexa Fluor 488-phalloidin (1:200 dilution) and 4',6-diamidino-2-phenylindole (DAPI, 1:5000 dilution) for 30 min in a humid chamber (37 °C). Immunofluorescence microscopy was conducted using a Zeiss Axiovert 200M inverted research-grade microscope (Carl Zeiss, Inc.), and immunofluorescence images were analyzed using ImageJ to measure the fluorescence intensity. For Oil Red O staining, after fixing cells, each sample stained with a lipid staining solution for adipogenesis (Oil Red O, Sigma) per manufacturer's instructions. Briefly, cells were incubated in 60% isopropanol for 5 min followed by immersion in Oil Red O working solution (3:2; 300 mg/mL Oil Red O in isopropanol:DI water) for 10 min to 1 h.

### 2.5. RNA isolation and RT-PCR

Adherent cells were lysed directly in TRIZOL reagent (Invitrogen) and total RNA was isolated by chloroform extraction and ethanol precipitation. Total RNA in DEPC water was amplified using TargetAmp™ 1-Round aRNA Amplification Kit 103 (Epicentre) according to vendor protocols. Total RNA was reverse transcribed using Superscript III® First Strand Synthesis System for RT-PCR (Invitrogen). RT-PCR was performed linearly by cycle number for each primer set using SYBR® Green Real-Time PCR Master Mix (Invitrogen) on an Eppendorf Realplex 4S Real-time PCR system. Primer sequences were as follows: C/EBP $\alpha$  — GCAAACCTACCCCTCCAATG and TTAGGTTCCAAGCCCCAAGT, PPAR2 — AGAGCCTTCCAACCTCCTCA and CAAG GCATTTCTGAAACCGA, LPL — CATCCCAITCACTCTGCCT and AGTTCTCCAATATCTA CCTCTGTG,  $\beta$ 3Tubulin — CCATTCTCGACTTTCCAAACCTG and CTGCGAACTTGCTT GTGGA, MAP2 — GGAGACAGAGATGAGAATTCCT and GAATTGGCTCTGACCTGGT, GAPDH — CTCTGCTCTCTGTTTCGAC and GTTCTCTCCGCCCTGTTTC. All reactions were performed linearly by cycle number for each set of primers.

## 3. Results

### 3.1. Hydrogel fabrication and single cell patterning

Previous reports of patterning on hydrogels used substrates of relatively high modulus ( $>2.5$  kPa) [23]. In order to study the combinatorial effects of cell shape, substrate stiffness and matrix composition in directing neurogenesis and adipogenesis on soft hydrogels ( $<1$  kPa), we developed a protocol based on soft lithography and chemically modified polyacrylamide (PAAm). Patterning ECM proteins on soft hydrogels via direct contact with an elastomeric stamp is challenging due to the substrate compliance and the presence of surface water, and few studies of microcontact printing on hydrogels have been reported [24]. Here we systematically varied curing, drying and contact times to identify an operating regime in which precise patterning of complex features on PAAm was possible (Fig. 1a). Polydimethylsiloxane (PDMS) stamps were prepared using photolithography to present geometric features in relief or flat surfaces without structure (unpatterned). Polyacrylamide (PAAm) hydrogels were prepared according to established literature methods [25], and we confirmed their stiffness ( $\sim 0.6$  kPa) via atomic force microscopy (AFM) (Fig. S1). The PAAm gels were treated with hydrazine hydrate and the stamps were inked with an oxidized glycoprotein solution to promote covalent immobilization after microcontact printing [26]. After seeding cells

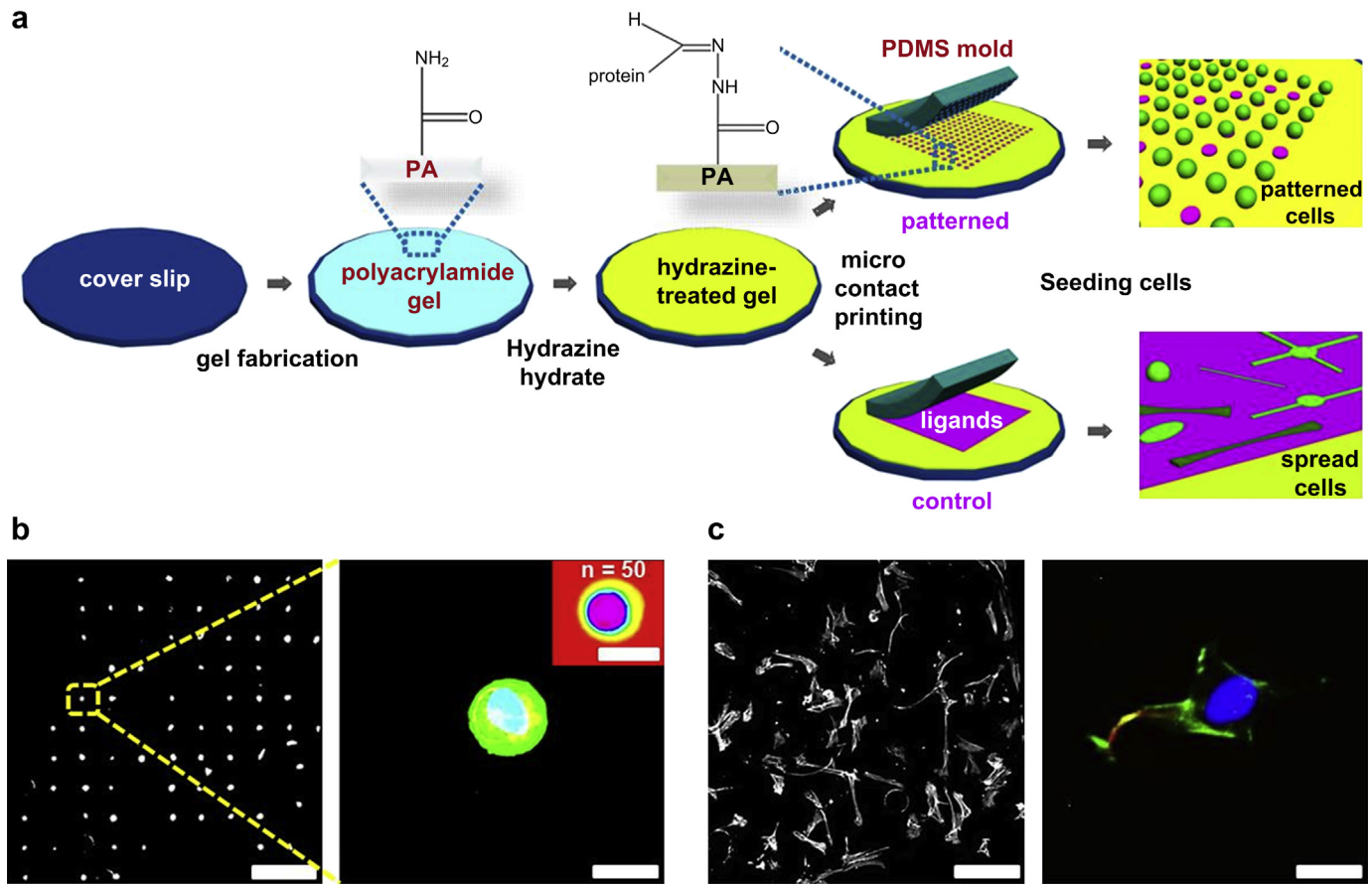


**Fig. 1.** Hydrazine-treated polyacrylamide enables protein immobilization and single cell patterning on soft hydrogels. (a) Schematic of the process used to pattern cells on polyacrylamide hydrogels. (b)–(c) Representative immunofluorescence microscopy images of MSCs cultured for 10 days: Inset shows a heat map of 50 different cells on small circular islands. Staining for MSC nuclei (blue), actin (cyan-green), p-par  $\gamma$  (yellow-green),  $\beta$ 3 tubulin (red). Scale bars: 700  $\mu\text{m}$  (left), 50  $\mu\text{m}$  (right). (For interpretation of the references to colour in this figure legend, the reader is referred to the web version of this article.)

on these surfaces, we confirmed that a substantial number of cells adhered to patterned regions (Fig. 1 and Fig. S2). Laser scanning confocal microscopy of patterned and unpatterned cells confirms that the average cell height is around 70  $\mu\text{m}$  and 15  $\mu\text{m}$  respectively (Fig. S3a). Morphological analysis reveals the average cell area is comparable to the desired pattern size (1000  $\mu\text{m}^2$ ) while the unpatterned cells show a variable spread area (1500  $\mu\text{m}^2$ –9500  $\mu\text{m}^2$ , Fig. S3b). Patterned cells remained viable and restricted to the islands for 13 days in culture, after which they escaped geometric confinement and proliferated (Fig. S4a).

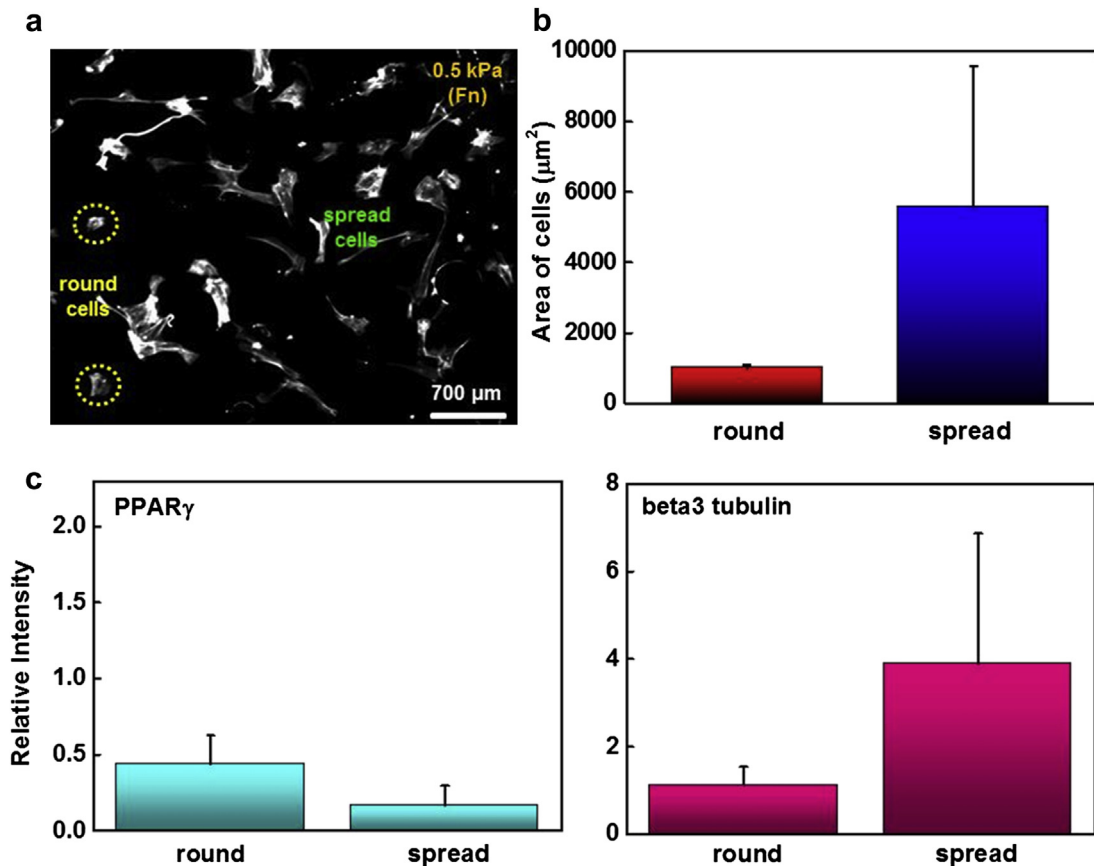
### 3.2. MSC differentiation on micropatterned soft hydrogels

Our initial analysis of MSCs on unpatterned soft gels showed a mixture of cells expressing markers associated with adipogenesis (p-par  $\gamma$ ) and neurogenesis (beta3 tubulin) (Fig. 2 and Fig. S4c). Cells that adopt a rounded, compact morphology express higher levels of adipogenesis markers while cells that spread and extend dendrite-like processes show elevated neurogenesis markers. We hypothesized that small isotropic geometries which restrict cell spreading may promote higher expression of adipogenesis markers compared to cells that are allowed to spread (Fig. 3a). To evaluate the temporal regulation of adipogenic and neurogenic marker expression, we cultured MSCs on fibronectin-coated islands and on unpatterned fibronectin-coated substrates for several weeks (Fig. S4b and c); protein expression was analyzed with histograms of intensities for patterned and unpatterned cells to assign

thresholds for designating lineage (Fig. S5). MSCs on small islands always showed higher levels of adipogenic marker expression relative to unpatterned cells regardless of time in cell culture while beta3 tubulin expression decreased dramatically after 10 days (Fig. S4b). Since MSCs cultured for 10 days showed clear distinction between the expressions of the two different markers, all further analysis was performed at 10 days in culture. The 1000  $\mu\text{m}^2$  patterned cells display high expression of p-par  $\gamma$  while the spread cells tend to express elevated beta3 tubulin (Fig. S4b and c). These results suggest that geometric confinement may prevent process extension — a hallmark characteristic of neuronal cells — and thus limit this differentiation potential. Restricting spreading may also enhance signaling associated with adipogenesis as has been observed previously [16].

### 3.3. MSC differentiation on micropatterned hydrogels with different matrix proteins

Since the early reports of MSCs undergoing neurogenesis on soft matrices used collagen as the adhesion protein [8], we next investigated whether different matrix proteins would influence the degree of adipogenesis and neurogenesis. Adipose tissue is comprised of a complex matrix containing collagen, laminin and fibronectin while brain tissue is predominantly composed of hyaluronan enmeshed with collagen and some laminin [27]. Therefore we investigated the degree of lineage specification for both programs when cells were adherent to combinations of these proteins.



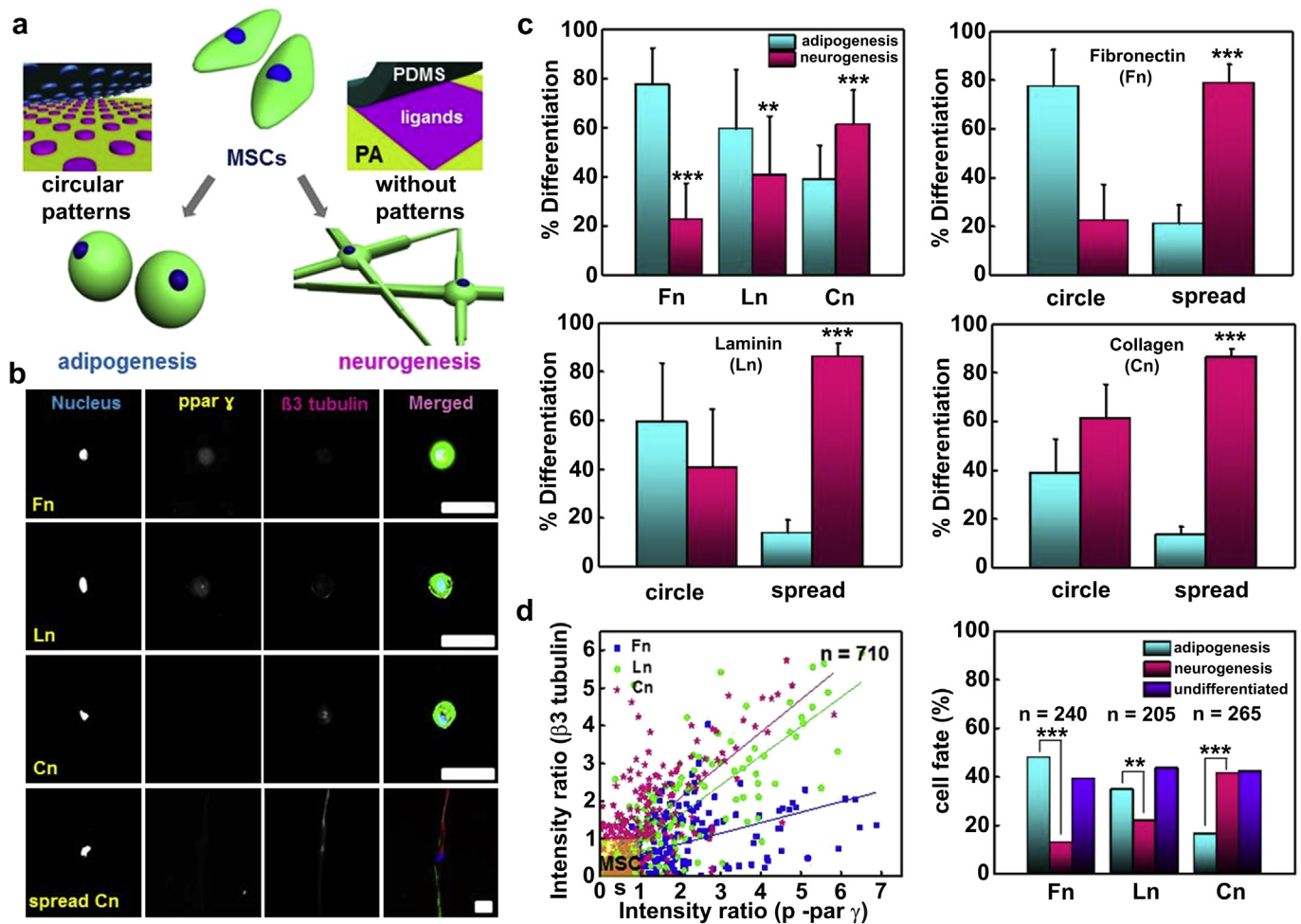
**Fig. 2.** Cell spreading influences the degree of adipogenic and neurogenic lineage specification. (a) Immunofluorescence image of MSCs adherent to the unpatterned fibronectin-coated substrates showing cells that display rounded morphology (10–20%). (b) Quantitation of average cell area for those in the population that display a rounded versus spread morphology. (c) Expression of adipogenic (left, p-par  $\gamma$ ) and neurogenic (right beta3 tubulin) markers in these populations demonstrating how spreading influences differentiation on soft hydrogel matrices. Error bars are standard deviations of over 70 cells per each condition.

Fig. 3b shows representative fluorescent images of MSCs cultured on small islands conjugated with fibronectin, laminin, and collagen. Across these different matrices, MSCs cultured on fibronectin display the highest expression of p-par  $\gamma$  while cells on collagen show the highest beta3 tubulin expression (Fig. 3c). MSCs cultured on laminin display intermediate expression of both markers. Quantitative analysis reveals that cells undergoing differentiation on the small fibronectin islands display nearly 80% adipogenic fate compared to 60% on laminin and 40% on collagen. In contrast, <20% of cells adherent to fibronectin islands are expressing beta3 tubulin compared to >40% on laminin and >60% on collagen. For all of the adhesion ligands, approximately 80% of the spread cells choose a neurogenic fate. Fig. 3d shows all data points we measured from five separate experiments with over 700 cells on small circular islands with the three different matrix proteins. We obtained intensity ratio via the comparisons with thresholds used to define lineage specification (Fig. S6) and describe populations of cells that display the adipocytes or neuronal stains or neither (Fig. 3d). Fitting lines of patterned cells on each matrix protein were produced using all data points; the trendline from fibronectin experiments corresponds to adipogenic specification while the trendline from collagen corresponds to the neurogenic specification. These results are comparable to that observed in percentages of round cells differentiating to adipocytes or neurons, which provides evidence that different matrix proteins have a strong influence on directing the differentiation of MSCs on these soft hydrogel matrices. Taken together, these results show that restricting cell spreading promotes adipogenesis regardless of ligand composition; however,

matrix composition in conjunction with cell geometry can further tailor the differentiation outcome.

To further verify the observed trends in differentiation, we performed immunofluorescence staining of the neurogenesis marker microtubule-associated protein 2 (MAP2) (Fig. S7), and histochemical analysis of accumulated lipid vacuoles using Oil Red O staining (Fig. S8). The lowest expression of MAP2 was observed with cells on small fibronectin islands while the highest expression was shown for spread cells on collagen. For Oil Red O staining, over 60% of cells in patterns expressed lipid droplets regardless of ligands compared to less than 40% in unpatterned cells. We also performed gene expression analysis using real-time polymerase chain reaction (PCR) of a panel of markers associated with adipogenesis (CEBPa and LPL) and neurogenesis (beta3 tubulin and MAP2). After 10 days in culture we see a higher degree of adipogenic transcript expression for micropatterned cells and higher expression of neurogenic transcripts in spread cells, consistent with the protein analysis using immunofluorescence and histology (Fig. 4). Patterned cells on fibronectin matrix showed ~10-fold enhanced expression of the adipogenic master regulator CEBPa compared to spread cells on fibronectin or laminin and ~20-fold higher expression than spread cells on collagen. The same trend was also observed in expression of lipoprotein lipase (LPL); patterned cells cultured on fibronectin, laminin and collagen displayed ~8-fold, ~6-fold, and ~40-fold enhancement in LPL expression respectively compared to unpatterned cells. In contrast, spread cells on collagen and laminin coated gels showed a ~10-fold increase in beta3 tubulin expression compared to ~2-fold





**Fig. 3.** Combinations of geometric features and adhesion ligands guide differentiation to adipocyte and neuronal lineages. (a) Schematic of MSC fate on soft PA hydrogels (0.6 kPa) with and without geometric constraints. (b) Representative immunofluorescence microscopy images of MSCs stained for p-par  $\gamma$  (yellow-green),  $\beta 3$  tubulin (red) cultured on PA hydrogels of various protein coating (fibronectin (Fn), laminin (Ln), and collagen (Cn)) with different shapes (round or spread) for 10 days; Scale bar: 70  $\mu\text{m}$ . (c) Percentage of cells captured on small circular islands or spread on the different matrix proteins, differentiating to adipocyte or neuronal lineages (\*\* $P < 0.005$ , \*\*\* $P < 0.0005$ , Fisher's exact test). (d) Plot of all measured immunofluorescence intensity data (cells cultured on small circular islands) divided by thresholds used to define lineage specification from five different experiments ( $n = 710$ ). The bar graph summarizes a distribution ratio from these cells (\*\* $P < 0.005$ , \*\*\* $P < 0.0005$ , Fisher's exact test). Error bars are standard deviations from five separate experiments with over 200 cells per shape and ligand. (For interpretation of the references to colour in this figure legend, the reader is referred to the web version of this article.)

increase on fibronectin. Similar trends were observed for MAP2 expression:  $\sim 3$ -fold for collagen and laminin and  $\sim 2$ -fold for fibronectin. These results reveal marked differences in gene expression associated with both cell geometry and matrix composition that corroborate the immunofluorescence results.

#### 3.4. The combined influence of geometric cues and matrix proteins

We have shown that cell spreading and the composition of adhesion ligand (fibronectin, laminin, and collagen) will influence MSC differentiation on soft hydrogels. To explore the role that cell spreading plays in guiding neurogenesis, we used microcontact printing of geometries that modulate cell area, aspect ratio and dendritic process extension. Fig. 5a and b shows representative immunofluorescence images of cells on circular features with different areas and anisotropic features after 10 days in culture. We observed that not only could smaller circular feature promote higher expression of adipogenesis markers (1000  $\mu\text{m}^2$  ( $\sim 75\%$ )  $> 3000 \mu\text{m}^2$  ( $\sim 63\%$ )  $> 5000 \mu\text{m}^2$  ( $\sim 51\%$ )), but also cells in anisotropic features such as 4-branched star and ovals (4:1 and 8:1 ratio) favored a neurogenic outcome (Fig. 5c). These anisotropic features allowed MSCs on soft hydrogels to spread and

extend processes, resulting in enhanced expression of neurogenic markers (about 85% for 8:1 oval) compared to round cells of the same area (3000  $\mu\text{m}^2$ , less than 40%). These trends were also shown for different adhesion ligands (laminin and collagen, Fig. S9), and we revealed a similar relation that cells confined to the same geometries but on different ligands showed a higher level of adipogenic (or neurogenic) expression on fibronectin (or collagen). An important outcome of these results is the demonstration that cell spreading promotes neuronal lineage specification irrespective of protein on the soft hydrogels. This suggests that spreading is necessary for the extension of dendritic processes and a requirement for initiation of neurogenic gene expression.

Since the composition of adhesion ligands can differentially regulate adipogenesis and neurogenesis, we compared differentiation of MSCs on various combinations of protein ligands at the same total concentration (Fig. 5d and Fig. S10). Patterned cells cultured on fibronectin or laminin matrices and a combination of both proteins tended to undergo adipogenesis. In sharp contrast, MSCs cultured on any combination of proteins containing collagen preferred to adopt a neurogenic outcome even on small circular islands (Fig. 5d). Unpatterned MSCs show a similar trend

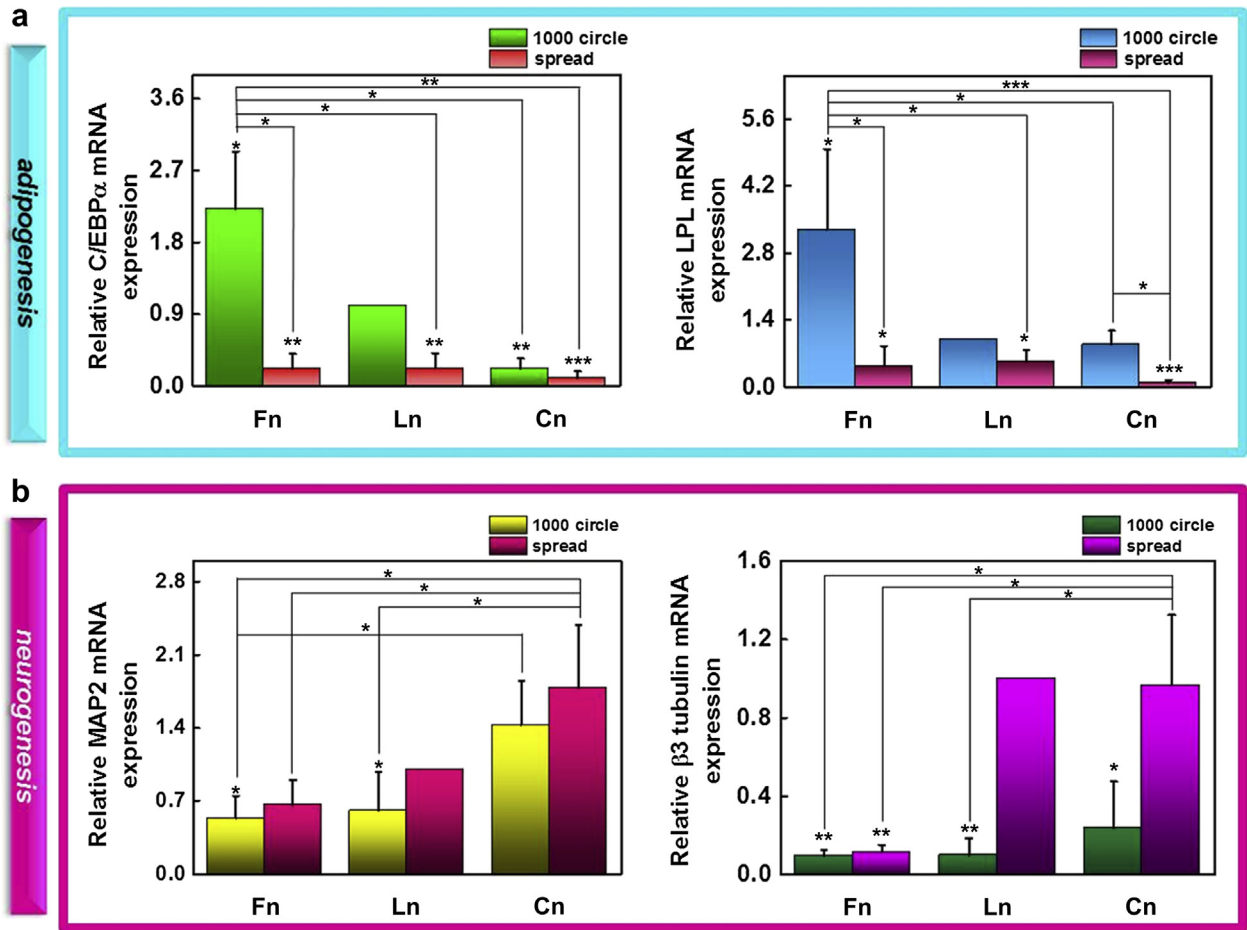


**Fig. 4.** Lineage-specific gene expression analysis of patterned and unpatterned mesenchymal stem cells. (a) Results of real-time PCR to measure the gene expression of C/EBP $\alpha$  and LPL as indicators of adipogenesis of MSCs (\* $P < 0.05$ , \*\* $P < 0.005$ , \*\*\* $P < 0.0005$ ,  $t$ -test). (b) Results of real-time PCR for quantitation of MAP2 and  $\beta 3$  tubulin as indicators of neurogenesis mRNA expression of MSCs (\* $P < 0.05$ , \*\* $P < 0.005$ ,  $t$ -test). Error bars are standard deviations from at least two separate experiments.

corresponding to matrix protein composition albeit with the majority of MSCs undergoing neurogenesis on account of spreading (Fig. S10).

### 3.5. MSC differentiation in pseudo-3D microenvironments

To explore whether our findings in the 2D screens could translate to a more physiologically relevant 3D system, we developed a templating approach to fabricate pseudo-3D microwells that vary geometry, stiffness and protein composition (Fig. 6a). Polyacrylamide gels were cast on the silicon master containing SU-8 photoresist using the same formulations chemistry described above. After polymerization the PAAm gel was subjected to hydrazine treatment and oxidized glycoprotein. To restrict the protein to the microwells, we removed surface protein with the use of adhesive tape to shear off the top layer of protein-conjugated gel. After seeding, cells only adhered within the microwell demonstrating the validity of this approach (Fig. 6b). After 10 days in culture MSCs encapsulated in the small circular fibronectin-coated microwells show equal expression of adipogenic and neurogenic markers. In contrast, cells encapsulated in high aspect ratio microwells show significantly higher expression of neurogenic markers. The decreased expression of adipogenic markers in the small pseudo-3D microwells is likely on account of the increased area the cell comes in contact with. Using the 1000  $\mu\text{m}^2$  template, the microwell depth will be  $\sim 15\text{--}20 \mu\text{m}$ , and the final adhesive area the encapsulated cell is exposed to will be  $\sim 2000 \mu\text{m}^2$ .

This result is consistent with the experiments that varied area (Fig. 5). The fraction of cells undergoing differentiation in either case is comparable to the 2D assays using the same geometric pattern, demonstrating the validity of this approach.

## 4. Discussion

The fate of mesenchymal stem cells cultured in soft hydrogel materials is controversial with literature demonstrating quiescence [28], neurogenesis [8,29,30], and adipogenesis (when cultured in the presence of differentiation media) [13,22,31]. The different outcomes in these studies are likely on account of differences in polymerization strategies, bioconjugation schemes and culture conditions. One commonality across these works is a variability in cell shape, where some cells extend dendrite-like processes while others fail to spread. To explore this further, we immunostained MSCs adherent to soft fibronectin-coated gels for markers associated with adipogenesis and neurogenesis and found a correlation between cell morphology and lineage marker expression. Round cells tend to express higher levels of adipogenesis markers while spread cells express higher levels of neurogenesis markers. This finding is significant because previous studies have only demonstrated adipogenesis on hydrogel materials in the presence of media supplements [13,22,31]. To discern whether cell shape may influence these different outcomes, we developed a micro-engineering platform to control single cell geometry on our hydrogel substrates. MSCs captured to small circular microislands

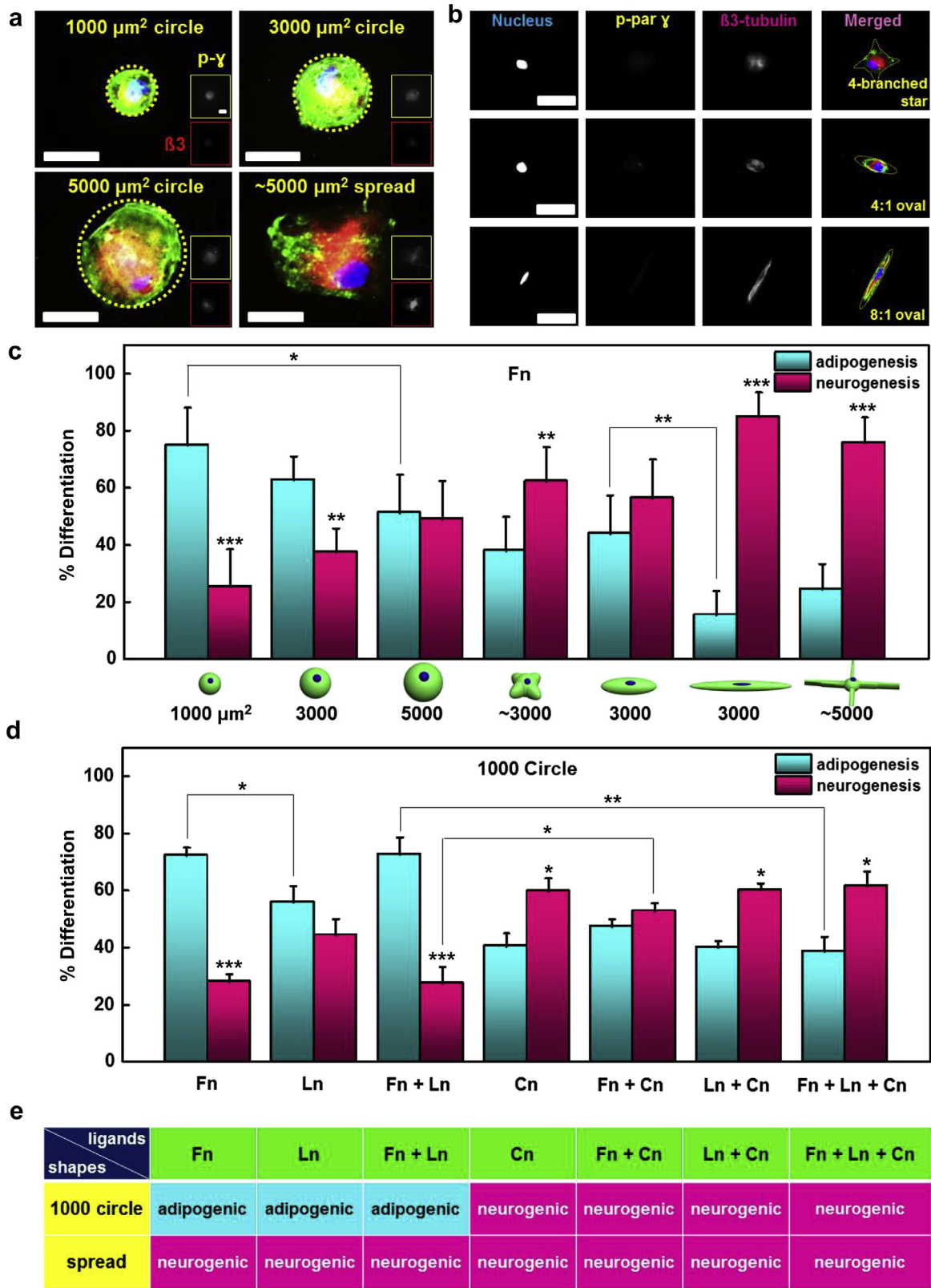


**Fig. 5.** Combining geometric cues and matrix protein composition to study adipogenesis and neurogenesis. (a)–(c) Representative immunofluorescence microscopy images of MSCs cultured in various microengineered geometries for 10 days. Variation in area (scale bar: 35  $\mu\text{m}$ ) and anisotropic geometric features (scale bar: 100  $\mu\text{m}$ ). Percentage of cells undergoing adipogenesis or neurogenesis when captured in fibronectin-coated geometric islands containing variable area, aspect ratio and branch points (\* $P < 0.05$ , \*\* $P < 0.005$ , \*\*\* $P < 0.0005$ , Fisher's exact test). (d) Percentage of cells on combination of different matrix proteins, fibronectin (Fn), laminin (Ln), or collagen (Cn), and combinations thereof (\* $P < 0.05$ , \*\* $P < 0.005$ , \*\*\* $P < 0.0005$ , Fisher's exact test). (e) Summary table demonstrating MSC fate decisions depending on the composition of matrix proteins (c and d). Error bars are standard deviations from three and two separate experiments with over 100 cells per each condition.

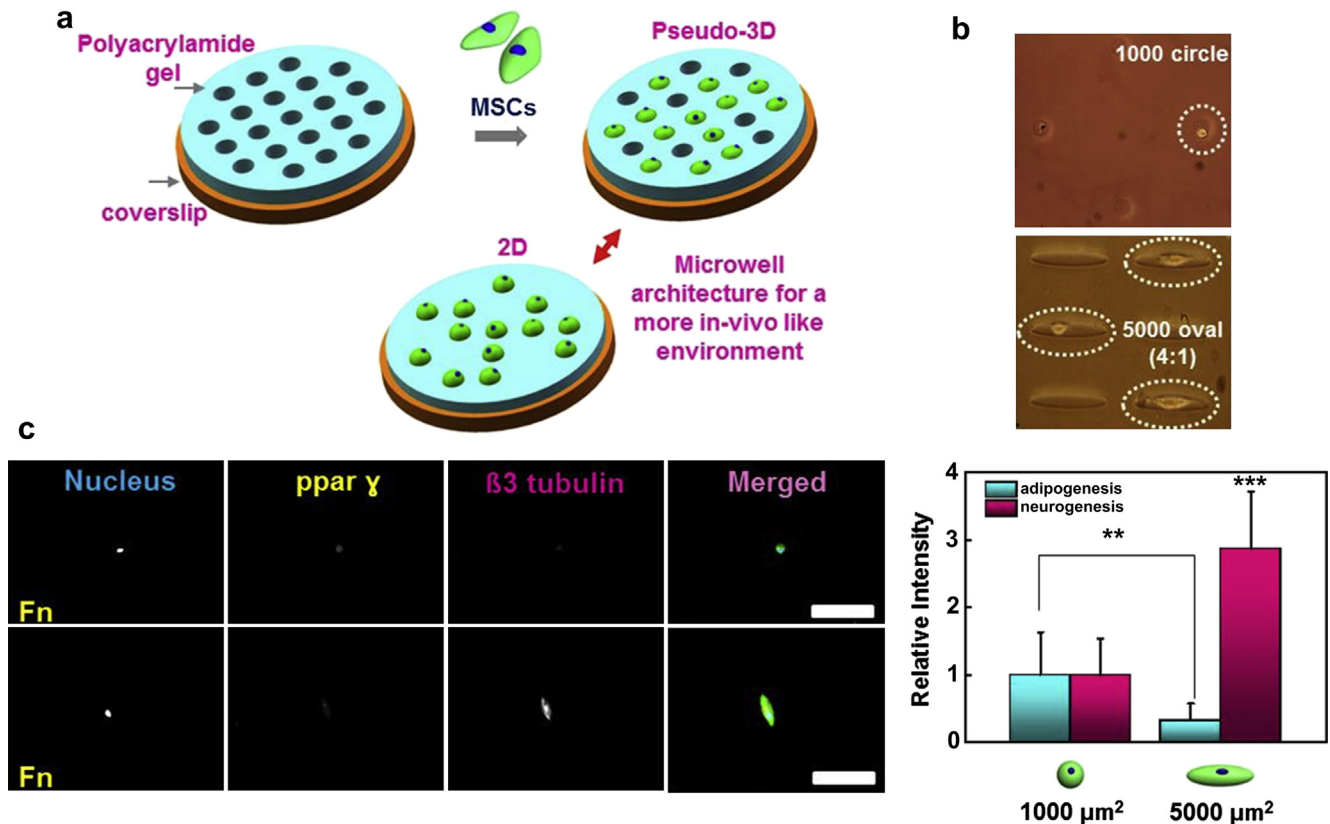


**Fig. 6.** Cells encapsulated in pseudo-3D microwells show a similar differentiation dependence to the 2D assays. (a) Schematic demonstrating the fabrication of protein-conjugated pseudo-3D microwells. (b) Photograph showing cells captured within the wells for small circular patterns and a high aspect ratio/high area geometry. (c) Left: immunofluorescence image of MSCs in the microwells stained for adipogenesis (p-par  $\gamma$ ) and neurogenesis ( $\beta$ 3 tubulin). Scale bar: 70  $\mu\text{m}$ . Right: quantitation of differentiation markers for a population of cells cultured in the microwell arrays.

express high levels of adipogenesis markers. MSCs that are induced to spread in anisotropic geometries — either directly on unpatterned gels or when patterned in shapes that vary cell area, aspect ratio and branching — display elevated expression of neurogenic markers. It is tempting to speculate that these geometric features relate to the in vivo morphological characteristics of these lineages — adipocytes show a characteristic isotropic morphology while neurons exhibit a branched dendritic phenotype. Nevertheless, it is clear that cell spreading is important for the extension of dendrite-like processes and initiation of neurogenic gene expression in adherent MSCs. In contrast, cells that are restricted from spreading prefer to initiate the adipogenesis program.

Another notable difference across previous studies is the composition of matrix protein grafted to the hydrogel. To explore the role of adhesion protein in guiding adipogenesis and neurogenesis, we covalently immobilized fibronectin, laminin and collagen to the PAAm hydrogels. MSCs cultured on fibronectin tend to express elevated adipogenic markers while MSCs on collagen tend to express elevated neurogenic markers. Gene expression analysis of key transcripts involved in regulating these differentiation potentials confirms the immunofluorescence results. This finding supports the early work that demonstrates primary neurogenesis of MSCs cultured on collagen coated PAAm [8]. In general, the extracellular matrix of neural tissue is enriched in hyaluronic acid (HA), collagen, and laminin. Schmidt et al. showed that Schwann cells prefer to differentiate into a neuronal phenotype when cultured in a 3D polymer matrix containing collagen [27]. In contrast, fibronectin is a significant component of adipose extracellular matrix [32] which suggests a specific role for this matrix protein in regulating adipogenesis in vivo.

Towards the identification of an optimal combination of cues for directing these different outcomes, we arrayed MSCs across geometries that vary area, aspect ratio and dendritic branch cues, with combinations of fibronectin, laminin and collagen grafted to the surface. Cells in fibronectin or laminin patterns preferred an adipogenesis fate while cells cultured on collagen matrices tended to show a high neurogenesis outcome regardless of geometry. This finding suggests that neurogenesis is the preferred lineage on collagen matrices, irrespective of cell shape, while restricting cell spreading promotes adipogenesis, particularly on matrices containing fibronectin. Thus, we hypothesize that the shape of stem and progenitor cells fostered by their microenvironment — and the composition of their surrounding adhesion proteins — are intimately connected to functional biological activity to direct or maintain cellular identity in vivo.

Previous studies have demonstrated that adhesion and associated signaling can be very different in 2D versus 3D environments [6]. To test the validity of our results in a more physiologically relevant 3D environment, we seeded MSCs within protein-conjugated microwells that were engineered to present the optimal geometry, stiffness and protein ligand discovered in our 2D assays. Cells that are encapsulated in large anisotropic microwells show enhanced neurogenesis compared to cells that are cultured within small isotropic microwells. This result is in-line with our 2D experiments and demonstrates the feasibility of translating these design criteria into pseudo-3D arrangements.

## 5. Conclusion

This study demonstrates that cell shape, matrix mechanics and the composition of adhesion protein all influence the lineage



specification in MSCs, individually and when presented together. Moreover, combining these cues can be used to maximize a desired differentiation outcome without the use of small molecule media supplements. Using this platform to combine physical and biochemical cues for directing other differentiation outcomes, and across other stem and progenitor cell types, may prove similarly revealing. Advances in controlling multiple cues reproducibly at the biomaterials interface and within 3D architectures will enable next generation assays that more closely recapitulate the structure of the in vivo environment. This work will prove useful in the design of tailored hydrogel biomaterials that more efficiently direct distinct differentiation outcomes.

## Disclosures

The authors indicate no potential conflicts of interest.

## Acknowledgements

This work was supported by start-up funding from the University of Illinois at Urbana-Champaign, College of Engineering, Department of Materials Science and Engineering.

## Appendix A. Supplementary data

Supplementary data related to this article can be found at <http://dx.doi.org/10.1016/j.biomaterials.2013.07.074>.

## References

- [1] Frith JE, Mills RJ, Hudson JE, Cooper-White JJ. Tailored integrin-extracellular matrix interactions to direct human mesenchymal stem cell differentiation. *Stem Cells Dev* 2012;21:2442–56.
- [2] Rowlands AS, George PA, Cooper-White JJ. Directing osteogenic and myogenic differentiation of MSCs: interplay of stiffness and adhesive ligand presentation. *Am J Physiol* 2008;295:C1037–44.
- [3] Kilian KA, Mrksich M. Directing stem cell fate by controlling the affinity and density of ligand-receptor interactions at the biomaterials interface. *Angew Chem Int Ed Engl* 2012;51:4891–5.
- [4] Guilak F, Cohen DM, Estes BT, Gimble JM, Liedtke W, Chen CS. Control of stem cell fate by physical interactions with the extracellular matrix. *Cell Stem Cell* 2009;5:17–26.
- [5] Higuchi A, Ling QD, Chang Y, Hsu ST, Umezawa A. Physical cues of biomaterials guide stem cell differentiation fate. *Chem Rev* 2013;113:3297–328.
- [6] Huebsch N, Arany PR, Mao AS, Shvartsman D, Ali OA, Bencherif SA, et al. Harnessing traction-mediated manipulation of the cell/matrix interface to control stem-cell fate. *Nat Mater* 2010;9:518–26.
- [7] Khetan S, Guvendiren M, Legant WR, Cohen DM, Chen CS, Burdick JA. Degradation-mediated cellular traction directs stem cell fate in covalently crosslinked three-dimensional hydrogels. *Nat Mater* 2013;12:1–8.
- [8] Engler AJ, Sen S, Sweeney HL, Discher DE. Matrix elasticity directs stem cell lineage specification. *Cell* 2006;126:677–89.
- [9] Keung AJ, Asuri P, Kumar S, Schaffer DV. Soft microenvironments promote the early neurogenic differentiation but not self-renewal of human pluripotent stem cells. *Integr Biol* 2012;4:1049–58.
- [10] Flanagan LA, Ju YE, Marg B, Osterfield M, Janney PA. Neurite branching on deformable substrates. *Neuroreport* 2002;13:2411–5.
- [11] Park SA, Shin JW, Yang YI, Kim YK, Park KD, Lee JW, et al. In vitro study of osteogenic differentiation of bone marrow stromal cells on heat-treated porcine trabecular bone blocks. *Biomaterials* 2004;25:527–35.
- [12] Saha K, Keung AJ, Irwin EF, Li Y, Little L, Schaffer DV, et al. Substrate modulus directs neural stem cell behavior. *Biophys J* 2008;95:4426–38.
- [13] Trappmann B, Gautrot JE, Connelly JT, Strange DG, Li Y, Oyen ML, et al. Extracellular-matrix tethering regulates stem-cell fate. *Nat Mater* 2012;11:642–9.
- [14] Hudalla GA, Murphy WL. Chemically well-defined self-assembled monolayers for cell culture: toward mimicking the natural ECM. *Soft Matter* 2011;7:9561–71.
- [15] Klim JR, Li L, Wrighton PJ, Piekarczyk MS, Kiessling LL. A defined glycosaminoglycan-binding substratum for human pluripotent stem cells. *Nat Methods* 2010;7:989–96.
- [16] McBeath R, Pirone DM, Nelson CM, Bhadriraju K, Chen CS. Cell shape, cytoskeletal tension, and RhoA regulate stem cell lineage commitment. *Dev Cell* 2004;6:483–95.
- [17] Kilian KA, Bugarija B, Lahn BT, Mrksich M. Geometric cues for directing the differentiation of mesenchymal stem cells. *Proc Natl Acad Sci U S A* 2010;107:4872–7.
- [18] Zhang D, Kilian KA. The effect of mesenchymal stem cell shape on the maintenance of multipotency. *Biomaterials* 2013;34:3962–9.
- [19] Peng R, Yao X, Ding J. Effect of cell anisotropy on differentiation of stem cells on micropatterned surfaces through the controlled single cell adhesion. *Biomaterials* 2011;32:8048–57.
- [20] Wilson A, Trumpp A. Bone-marrow haematopoietic-stem-cell niches. *Nat Rev Immunol* 2006;6:93–106.
- [21] Janney PA, Miller RT. Mechanisms of mechanical signaling in development and disease. *J Cell Sci* 2011;124:9–18.
- [22] Fu J, Wang YK, Yang MT, Desai RA, Yu X, Liu Z, et al. Mechanical regulation of cell function with geometrically modulated elastomeric substrates. *Nat Methods* 2010;7:733–6.
- [23] Aydin D, Louban I, Perschmann N, Blümmel J, Lohmüller T, Cavalcanti-Adam EA, et al. Polymeric substrates with tunable elasticity and nanoscopically controlled biomolecule presentation. *Langmuir* 2010;26:15472–80.
- [24] Hynd MR, Frampton JP, Dowell-Mesfin N, Turner JN, Shain W. Directed cell growth on protein-functionalized hydrogel surfaces. *J Neurosci Methods* 2007;162:255–63.
- [25] Tse JR, Engler AJ. Preparation of hydrogel substrates with tunable mechanical properties. *Curr Protoc Cell Biol* 2010;47:10.16.1–10.16.16.
- [26] Damjanović V, Lagerholm BC, Jacobson K. Bulk and micropatterned conjugation of extracellular matrix proteins to characterized polyacrylamide substrates for cell mechanotransduction assays. *Biotechniques* 2005;39:847–51.
- [27] Suri S, Schmidt CE. Cell-laden hydrogel constructs of hyaluronic acid, collagen, and laminin for neural tissue engineering. *Tissue Eng Part A* 2010;16:1703–16.
- [28] Winer JP, Janney PA, McCormick ME, Funaki M. Bone marrow-derived human mesenchymal stem cells become quiescent on soft substrates but remain responsive to chemical or mechanical stimuli. *Tissue Eng Part A* 2009;15:147–54.
- [29] Banerjee A, Arha M, Choudhary S, Ashton RS, Bhatia SR, Schaffer DV, et al. The influence of hydrogel modulus on the proliferation and differentiation of encapsulated neural stem cells. *Biomaterials* 2009;30:4695–9.
- [30] Reilly GC, Engler AJ. Intrinsic extracellular matrix properties regulate stem cell differentiation. *J Biomech* 2010;43:55–62.
- [31] Park JS, Chu JS, Tsou AD, Diop R, Tang Z, Wang A, et al. The effect of matrix stiffness on the differentiation of mesenchymal stem cells in response to TGF- $\beta$ . *Biomaterials* 2011;32:3921–30.
- [32] Mariman EC, Wang P. Adipocyte extracellular matrix composition, dynamics and role in obesity. *Cell Mol Life Sci* 2010;67:1277–92.